THE USE OF THE EIT PRINCIPLES FOR THE "IN VIVO" MEASUREMENT OF THE ELECTRIC RESISTIVITIES OF BRAIN, SKULL AND SCALP.

S.Gonçalves[1,2], J.C. de Munck[1], J.P.A. Verbunt[1], F. Bijma[1]
[1]MEG Centre VUMC, Vrije Universiteit, Amsterdam, The Netherlands
[2]Institute of Biophysics and Biomedical Engineering, University of Lisbon, Lisbon, Portugal

Abstract - **The goal of this work is to perform the "in vivo" measurement of equivalent electric resistivities of skull (ρ_{skull}) and brain (ρ_{brain}) using an Electric Impedance Tomography (EIT) based method and realistic models for the head. Results demonstrate that $\rho_{skull}/\rho_{brain}$ is more likely to be within 20 and 50 rather than equal to the commonly accepted value of 80. The variation in ρ_{brain} (average=301 Ω.cm, SD=13%) and ρ_{skull} (average=12230 Ω.cm, SD=18%) is decreased by half, when compared to the results using the sphere model, showing that the correction for geometry errors is essential to obtain realistic estimations for the resistivities. Earlier results show the necessity of calibrating ρ_{brain} and ρ_{skull}, by measuring them "in vivo" for each subject, in order to decrease errors associated with the EEG Inverse Problem (IP). We show that the proposed method is suited to this goal.**

I. INTRODUCTION

The Inverse Problem (IP) [1] of EEG aims to determine the sources inside the brain that best explain the electrical potentials measured on the surface of the scalp. The determination of the sources is made through the use of mathematical models, which describe the head as an electrical conductor. In this way, the knowledge of the electrical conductivities of the tissues of the head must be known a priori and it is known that the solution to the EEG IP is highly dependent on the values taken for these parameters [2, 3]. The first attempts to measure the electrical conductivities of the tissues were made "in vitro" and often using animal tissue samples. These measurement procedures are affected of large systematic errors. As a consequence, the values presented in literature for the electrical conductivities show a wide range of variation and there might be a factor of 7 between the minimum and maximum conductivity values reported for a certain tissue [4, 5]. Recently, several studies have been performed to try to estimate "in vivo" the electrical conductivities of several head structures. Some approaches like the one in [6] use the Boundary Element Method (BEM) and realistic head models to estimate the equivalent electrical resistivities of brain, skull and skin. In the present work, "in vivo" measurements of the electrical resistivities of brain (ρ_{brain}), skull (ρ_{skull}) and scalp (ρ_{scalp}) are performed for 6 different subjects, using the approaches described in [2, 7]. However, differently from [7], realistic models instead of spherical models are used to describe the head and the BEM is used to solve the forward problem of EIT.

In order to avoid biased estimations of the electrical resistivities, a thorough study is performed to determine the optimal conditions yielding the lowest possible BEM numerical error for EIT. Furthermore, the mathematical problem of using the BEM for many combinations of electrical resistivities although using the same geometry is analysed and optimised using the Sherman-Morrison-Woodbury formula [8].

II. METHODOLOGY

A. EIT Method

In the BEM formulation [9-12] the volume conductor is described by a set of homogeneous, isotropic and non-intersecting compartments, of arbitrary shape, each one characterised by a certain electrical conductivity. It is considered that there are no sources inside the volume and the electrical current enters or leaves the conductor only through electrodes placed on the outer surface. In this study, the volume conductor consists of 3 nested compartments representing, from outer to inner compartment, scalp, skull and brain. In this case, the potential generated on a certain point $\vec{\mathbf{r}}_p$ on the surface of the conductor by an injected current density $\vec{\mathbf{J}}(\vec{\mathbf{r}}')$ will be given by the integral equation [13]:

$$\sigma_p \Psi(\vec{\mathbf{r}}_p) = \frac{1}{4\pi}\sum_{i=0}^{2}(\sigma_i^- - \sigma_i^+)\oint_{S_i}\Psi(\vec{\mathbf{r}})\,d\omega_i - \frac{1}{4\pi}\oint_{S_0}\frac{\vec{\mathbf{J}}(\vec{\mathbf{r}})\cdot\vec{\mathbf{n}}_0}{|\vec{\mathbf{r}}-\vec{\mathbf{r}}_p|}\,dS \qquad (1)$$

where

σ_p is the conductivity of the outer compartment;

σ_i^- is the inner conductivity of compartment **i**;

σ_i^+ is the outer conductivity of compartment **i**;

S_i is the surface delimiting compartment **i**;

$\vec{\mathbf{n}}_0$ is the normal to surface S_0;

$d\omega_i$ is the solid angle of the elemental surface dS_i as seen from $\vec{\mathbf{r}}_p$.

Furthermore, the BEM approach assumes the discretisation of the surfaces into a set of triangles whose vertices are the nodes of the surface. When the potential is linearly interpolated over triangles, the potential measured on a certain node **i** of surface S_m is written as:

$$\sigma_m \Psi_i^m = \frac{1}{4\pi}\sum_{k=0}^{2}\sum_{j=0}^{N_k-1}(\sigma_k^- - \sigma_k^+)\Omega_{ij}^{mk}\Psi_j^k - \frac{1}{4\pi}(\Gamma_{i1}J_{n,1} - \Gamma_{i2}J_{n,2}) \qquad (2)$$

where

N_k is the number of nodes of surface **k**;

Ω_{ij}^{mk} is the linearly weighted solid angle viewed from $\vec{\mathbf{r}}_i$ on surface m, of the direct neighbouring triangles of point $\vec{\mathbf{r}}_j$ on surface k [9];

Γ_{i1} and Γ_{i2} are the integrals of $\frac{1}{\left|\vec{\mathbf{r}}-\vec{\mathbf{r}}_p\right|}$ over the surface element dS_0 respectively associated to injection electrode 1 and 2 and it is defined according to [9] .

$J_{n,j}=\left(\vec{\mathbf{J}}\cdot\vec{\mathbf{n}}_0\right)_j$ is the current density at triangle j of surface S_0 where j=1,2. The original triangle is shrunk by a factor of 0.9 and the current density is calculated over the area of the new triangle to avoid singularity problems when the view point is coincident with one of the three corners;

After some manipulations, (2) can be written in matrix form as:

$$\mathbf{A\Psi=\Gamma J} \qquad (3)$$

where

A is the N×N system matrix containing the equation dependence on the electrical conductivities. N is the total number of nodes of the 3 surfaces and each matrix element is defined as:

$$A_{ij}^{mk}=\sigma_m\delta_{ij}^{mk}-\frac{1}{4\pi}\left(\sigma_k^-+\sigma_k^+\right)\Omega_{ij}^{mk}\ ; \qquad (4)$$

Ψ is the N×1 column vector containing the potential values;

Γ is the N×2 matrix containing the integrals Γ_{ij}, where j=1, 2;

J is the 2×1 column vector containing the current density values.

Since the solution of (3) is determined up to an arbitrary constant, the system matrix **A** has to be deflated to obtain uniqueness. In this paper, the deflated matrix **M** is defined as:

$$\mathbf{M}=\mathbf{A}+\frac{\mathbf{ee}^T}{N} \qquad (5)$$

where **e** is an N×1 vector of ones.

The inverse problem of EIT is solved through the minimisation of the cost function defined in [2] and assuming, as in previous studies [2, 6, 7, 14], that $\sigma_{brain}=\sigma_{scalp}$:

$$\mathrm{Cost}\left(\sigma_{brain},\frac{\sigma_{skull}}{\sigma_{brain}}\right)=\frac{\sum_{k,i}\left(\Psi_{ik}-\tilde{\Psi}_{ik}\right)^2}{\sum_{k,i}\left(\Psi_{ik}\right)^2} \qquad (6)$$

where

i runs over the number of measuring electrode pairs;

k runs over the number of injection electrode pairs;

Ψ_{ik} is the potential measured by electrode pair i and generated by injection electrode pair k;

$\tilde{\Psi}_{ik}$ is the potential predicted on measuring electrode pair i and generated by injection electrode pair k.

The forward problem of EIT must be solved in order to obtain the model potential $\tilde{\Psi}_{ik}$. This is accomplished through the solution of equation (3) in order to find Ψ. However, the adjustment of the electrical conductivities implies the re-computation of the system matrix **A** and the solution of equation (3) for each one of the iterations, which increases enormously the computational burden. In order to simplify this task, attention was focused on the simplification of matrix **A**, containing the dependence on the electrical conductivities. It can be shown [14] that the system matrix **A** can be written as:

$$\mathbf{A}=\tilde{\mathbf{A}}\,\mathbf{\Lambda_1}+\mathbf{\Lambda_2} \qquad (7)$$

where

$\tilde{\mathbf{A}}$ is the system matrix with σ_0 and the conductivity differences set to unity;

$\mathbf{\Lambda_1}$ is the $N\times N$ diagonal matrix defined as:

$$\Lambda_1=\mathrm{diag}\left(-\sigma_0,\ldots,-\sigma_0,(\sigma_0-\sigma_1),\ldots,(\sigma_0-\sigma_1),(\sigma_1-\sigma_2),\ldots,(\sigma_1-\sigma_2)\right) \qquad (8)$$

where $N=N_0+N_1+N_2$ and each constant is respectively repeated N_0, N_1 and N_2 times.

$\mathbf{\Lambda_2}$ is the $N\times N$ diagonal matrix defined as:

$$\Lambda_2=\mathrm{diag}\left(0,\ldots,0,(2\sigma_0-\sigma_1),\ldots,(2\sigma_0-\sigma_1),(3\sigma_1-2\sigma_2),\ldots,(3\sigma_1-2\sigma_2)\right) \qquad (9)$$

where each constant is respectively repeated N_0, N_1 and N_2 times.

The constants N_0, N_1 and N_2 are the number of nodes of surfaces S_0, S_1 and S_2, corresponding to scalp, skull and brain and their sum equals the total number of nodes N. The parameters σ_0, σ_1, and σ_2 are respectively the inner conductivities of scalp, skull and brain.

The decomposition of matrix **A** as presented in (7) allows the optimisation of the computation of **Ψ** since the geometrical integrals are stored in memory, thus being computed only once. Furthermore, the Sherman-Morrison-Woodbury formula can be applied. The advantage of the application of the Sherman-Morrison formula is to reduce the size of the matrix to be inverted with the consequent saving of computation time. In these circumstances, the computation time on a Pentium PC with a 200 MHz CPU and 128 MB of RAM was approximately equal to 3 hours.

B. Head Models

The head was described using a set of 3 nested compartments, representing respectively the scalp, the skull and the brain. The shape of the compartments was derived from the segmentation of brain, skull and scalp obtained from the MRI scans of each patient. For five of the subjects, the segmentation was obtained using the automatic method described in [15]. For subject 5 segmentation was obtained using Curry Version 3.0 (Neurosoft, Inc.), since the results obtained with the aforementioned method were not entirely satisfactory in what regards the shape of the brain, skull and scalp compartments as well as the skull thickness.

The point distribution among the 3 surfaces depends on the conditions yielding the lowest numerical error associated to the BEM model. This corresponds to allocate 60% of the points to the scalp, 30% of the points to the skull and 10% of the points to the brain [14]. A local refinement of the grid was applied around the injection electrodes, in the case of the EIT method since it increased BEM's numerical accuracy. The total number of

points used in the discretization of the 3 surfaces was set approximately equal to 3000.

III. DATA ACQUISITION

The same data as in [7] were used in the present study. The data acquisition from 6 normal subjects was performed using the Omega MEG/EEG system (CTF Systems Inc.), with 64 electrodes positioned according to the extended 10-20 system. Electrode positions were determined according to the method described in [16]. Current was injected on a pair of electrodes while measuring the potential distribution on the remaining sensors, this procedure being repeated for several injection pairs. As explained in [7] the injection and extracting electrodes were positioned with a maximum separation in between them, and the reference electrode located approximately halfway between injection and extracting electrodes. Furthermore the injection-extraction electrode pairs were chosen to cover the entire perimeter of the head and their number varied between 7 and 10. Data were acquired at a rate of 1250 Hz, using on-line high and low-pass filters at 0.16 Hz and 300 Hz respectively. Epochs of 105 seconds were recorded for each injection pair, each epoch consisting of 32 trials of 3.28 seconds, recorded in sequence. Data pre-processing was performed according to [7].

IV. RESULTS

For each subject the equivalent electrical resistivities were computed using the EIT method. Local refinement was applied around the injection electrodes and the refinement distance is varied in such a way that the total number of points used in the BEM model (app. 3000 points) is comparable among subjects. The obtained results are presented in Table I. In fig. 1 a scatterplot of ρ_{skull} against ρ_{brain} is presented containing data from the six subjects. The same scatterplot obtained using the spherical model [7] is represented in the same graph for comparison.

In Table I it is seen that for subjects 1 to 5 the values of $\rho_{skull}/\rho_{brain}$, ρ_{brain} and ρ_{skull} are very similar and in particular the variability in the resistivity of the skull is small. The results regarding subject 6 differ slightly from those obtained for the other subjects such that the values concerning $\rho_{skull}/\rho_{brain}$ and ρ_{skull} are slightly lower. The observation of fig. 1 allows the comparison between the variability in the values of ρ_{brain} and ρ_{skull} for spherical [7] and realistic models. It can be seen that there is a clear trend of decrease in the variation (ratio between maximum and minimum values) of ρ_{brain} and ρ_{skull} when using realistic models. Taking as an example the values of ρ_{skull}, in the case of the spherical model the variation is even slightly higher than a factor of 2. In the case of the realistic models, this variation decreases to a factor of 1.75 if subject 6 is included or to a factor of 1.19 if subject 6 is not included.

Subject	ρ_{brain}(Ω.cm)	ρ_{skull}(Ω.cm)	$\rho_{skull}/\rho_{brain}$
1	333	11928	36
2	292	12344	42
3	292	14217	49
4	311	13598	44
5	234	13174	56
6	346	8119	23
Average	301	12230	42
SD (%)	13	18	27

Table I - Resistivity estimations obtained with the EIT method using realistic models. In addition the average of ρ_{brain} and ρ_{skull} as well as the corresponding relative standard deviations (SD) are also presented.

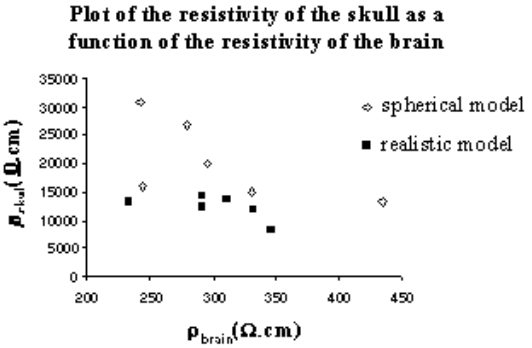

Fig. 1 - Plot of the resistivity of the skull as a function of the resistivity of the brain, obtained with the EIT method using both spherical and realistic models. The results of the spherical model were obtained are presented in [7].

V. DISCUSSION AND CONCLUSIONS

The results presented in this paper show the feasibility of the proposed EIT method to perform "in vivo" estimations of $\rho_{skull}/\rho_{brain}$, ρ_{skull} and ρ_{brain} using realistic models for the head. The results also show that the ratio between the resistivities of skull and brain is more likely to be in the range of 20 to 50 rather than equal to the commonly accepted value of 80. Another important point is related to the fact that, even with head geometry correction, there are still variations to be accounted for, thus pointing to the necessity of calibrating the values of $\rho_{skull}/\rho_{brain}$, ρ_{skull} and ρ_{brain} by measuring them "in vivo" for each subject. We think that the proposed EIT method is not only able to fulfil this goal but also has technical requirements usually available in any EEG laboratory.

REFERENCES

[1] Barber, D.C. and B.H. Brown, *Applied potential tomography*. J. Phys. E.: Sci Instrum., 1984. **37**: p. 723-732.

[2] Gonçalves, S., et al., *The application of electrical impedance tomography to reduce systematic errors in the EEG inverse problem--a simulation study.* Physiol Meas, 2000. **21**(3): p. 379-93.

[3] Koles, Z.J., *Trends in EEG source localization.* Electroencephalogr Clin Neurophysiol, 1998. **106**(2): p. 127-37.

[4] Faes, T.J., et al., *The electric resistivity of human tissues (100 Hz-10 MHz): a meta-analysis of review studies.* Physiol Meas, 1999. **20**(4): p. R1-10.

[5] Geddes, L.A. and L.E. Baker, *The specific resistance of biological material--a compendium of data for the biomedical engineer and physiologist.* Med Biol Eng, 1967. **5**(3): p. 271-93.

[6] Oostendorp, T.F., J. Delbeke, and D.F. Stegeman, *The conductivity of the human skull: results of in vivo and in vitro measurements.* IEEE Trans Biomed Eng, 2000. **47**(11): p. 1487-92.

[7] Gonçalves, S., et al., *In vivo measurement of the Brain and Skull resistivities using an EIT based method and the combined analysis of SEF/SEP data.* IEEE Trans Biomed Eng, submitted, 2001.

[8] Press, W.H., et al., *Numerical Recipes in C*. 1988, Cambridge: Cambridge University Press.

[9] de Munck, J.C., *A linear discretization of the volume conductor boundary integral equation using analytically integrated elements.* IEEE Trans Biomed Eng, 1992. **39**(9): p. 986-90.

[10] Mosher, J.C., R.M. Leahy, and P.S. Lewis, *EEG and MEG: forward solutions for inverse models.* IEEE Trans Biomed Eng, 1999. **46**(3): p. 245-59.

[11] Oostendorp, T.F. and A. van Oosterom, *Source parameter estimation in inhomogeneous volume conductors of arbitrary shape.* IEEE Trans Biomed Eng, 1989. **36**(3): p. 382-91.

[12] Hamalainen, M.S. and J. Sarvas, *Realistic conductivity geometry model of the human head for interpretation of neuromagnetic data.* IEEE Trans Biomed Eng, 1989. **36**(2): p. 165-71.

[13] Oostendorp, T. and A. van Oosterom, *The potential distribution generated by surface electrodes in inhomogeneous volume conductors of arbitrary shape.* IEEE Trans Biomed Eng, 1991. **38**(5): p. 409-17.

[14] Gonçalves, S., et al., *In vivo measurement of the Brain and Skull resistivities using an EIT based method and realistic models for the head.* IEEE Trans Biomed Eng, submitted, 2002.

[15] van't Ent, D., J.C. de Munck, and A.L. Kaas, *A fast method to derive realistic BEM models for E/MEG source reconstruction.* IEEE Trans Biomed Eng, 2001. **48**(12): p. 1434-43.

[16] de Munck, J.C., et al., *The use of an MEG device as 3D digitizer and motion monitoring system.* Phys Med Biol, 2001. **46**(8): p. 2041-52.